

Git Re-Basin: Merging Models modulo Permutation Symmetries

Samuel K. Ainsworth

skainswo@cs.washington.edu

Jonathan Hayase

jhayase@cs.washington.edu

Siddhartha Srinivasa

siddh@cs.washington.edu

*School of Computer Science and Engineering
University of Washington*

Abstract

The success of deep learning is thanks to our ability to solve certain massive non-convex optimization problems with relative ease. Despite non-convex optimization being NP-hard, simple algorithms – often variants of stochastic gradient descent – exhibit surprising effectiveness in fitting large neural networks in practice. We argue that neural network loss landscapes contain (nearly) a single basin, after accounting for all possible permutation symmetries of hidden units. We introduce three algorithms to permute the units of one model to bring them into alignment with units of a reference model. This transformation produces a functionally equivalent set of weights that lie in an approximately convex basin near the reference model. Experimentally, we demonstrate the single basin phenomenon across a variety of model architectures and datasets, including the first (to our knowledge) demonstration of zero-barrier linear mode connectivity between independently trained ResNet models on CIFAR-10 and CIFAR-100. Additionally, we identify intriguing phenomena relating model width and training time to mode connectivity across a variety of models and datasets. Finally, we discuss shortcomings of a single basin theory, including a counterexample to the linear mode connectivity hypothesis.

1 Introduction

We investigate the unreasonable effectiveness of stochastic gradient descent (SGD) algorithms on the high-dimensional non-convex optimization problems of deep learning. In particular, we are motivated by three questions:

1. Why does SGD thrive in the optimization of high-dimensional non-convex deep learning loss landscapes, despite being noticeably less robust in other non-convex optimization settings like policy learning (Ainsworth et al., 2021), trajectory optimization (Kelly, 2017), and recommender systems (Kang et al., 2016)?
2. Where are all the local minima? When linearly interpolating between initialization and final trained weights, why does the loss smoothly, monotonically decrease (Goodfellow & Vinyals, 2015; Frankle, 2020; Lucas et al., 2021; Vlaar & Frankle, 2021)?
3. How is it that two independently trained models with different random initializations and data batch orders inevitably achieve nearly identical performance? Furthermore, why do their training loss curves look identical?

We argue that this final phenomenon points to the existence of some yet uncharacterized invariance(s) in the training dynamics, such that independent training runs exhibit near identical characteristics. Brea et al.

ARCHITECTURE	NUM. PERMUTATION SYMMETRIES
MLP (3 layers, 512 width)	$10 \wedge 3498$
VGG16	$10 \wedge 35160$
ResNet50	$10 \wedge 55109$
Atoms in the observable universe	$10 \wedge 82$

Table 1: Permutation symmetries of deep learning models vs. an upper estimate on the number of atoms in the known, observable universe. Deep learning loss landscapes contain incomprehensible amounts of geometric repetition.

(2019) noted the permutation symmetries of hidden units in neural networks. Briefly: one can swap any two units of a hidden layer in a network and – assuming weights are adjusted accordingly – the functionality of the network will remain unchanged. Recently, Entezari et al. (2021) conjectured that these permutation symmetries may allow us to linearly connect points in weight space with no detriment to the loss.

Conjecture 1 (Permutation invariance, informal (Entezari et al., 2021)). Most SGD solutions belong to a set whose elements can be permuted in such a way that there is no barrier (as in Definition 2.2) on the linear interpolation between any two permuted elements.

We refer to such solutions as being *linearly mode connected* (LMC) (Frankle et al., 2020). If true, Conjecture 1 has the potential to materially expand our understanding of how SGD works in the context of deep learning, and offers a credible explanation for these three phenomenon in particular.

Contributions. In this paper, we attempt to uncover what invariances may be responsible for these three phenomena and the unreasonable effectiveness of SGD in deep learning. We make the following contributions:

1. **Matching methods.** We propose three novel algorithms to align the weights of two independently trained models, grounded in concepts and techniques from combinatorial optimization. Where appropriate, we prove hardness results for these problems and propose approximation algorithms. Our fastest method identifies permutations in mere seconds on current hardware.
2. **Relationship to SGD.** We demonstrate by means of counterexample that linear mode connectivity is an emergent property of SGD training, as opposed to model architectures. We connect this result to prior work on the implicit biases of SGD.
3. **Experiments, including zero-barrier LMC for realistic ResNets.** Empirically, we explore the existence of linear mode connectivity modulo permutation symmetries in experiments across MLPs, CNNs, and ResNets trained on MNIST, CIFAR-10, and CIFAR-100. We contribute the first-ever demonstration of zero-barrier LMC between two independently trained ResNet models on non-trivial datasets. We explore the relationship between LMC and model width, as well as training time. Finally, we exhibit our methods’ ability to combine models trained on independent datasets into a merged model that outperforms both input models and is no more expensive in compute or memory than either of the input models.

2 Background

Although our methods can be applied to arbitrary model architectures, we will proceed with the multi-layer perceptron (MLP) architecture for its ease of presentation (Bishop, 2007). We consider models following an L -layer MLP architecture,

$$f(\mathbf{x}; \Theta) = \mathbf{z}_{L+1}, \quad \mathbf{z}_{\ell+1} = \sigma(\mathbf{W}_\ell \mathbf{z}_\ell + \mathbf{b}_\ell), \quad \mathbf{z}_1 = \mathbf{x}$$

where σ denotes an element-wise nonlinear activation function. Furthermore, we consider a loss, $\mathcal{L}(\Theta)$, measuring the suitability of a particular set of weights Θ towards some goal, say fitting to a training dataset.

Central to our investigation is the phenomenon of *permutation symmetries* of weight space. Given Θ we can take any intermediate layer, ℓ , of the model and apply some permutation to its output features, denoted by a permutation matrix $\mathbf{P} \in S_d$,¹

$$\mathbf{z}_{\ell+1} = \mathbf{P}^\top \mathbf{P} \mathbf{z}_{\ell+1} = \mathbf{P}^\top \mathbf{P} \sigma(\mathbf{W}_\ell \mathbf{z}_\ell + \mathbf{b}_\ell) = \mathbf{P}^\top \sigma(\mathbf{P} \mathbf{W}_\ell \mathbf{z}_\ell + \mathbf{P} \mathbf{b}_\ell)$$

for σ an element-wise operator. It follows that as long as we reorder the input weights of layer $\ell+1$ according to \mathbf{P}^\top , we will have a functionally equivalent model. To be precise, if we define Θ' to be identical to Θ with the exception of

$$\mathbf{W}'_\ell = \mathbf{P} \mathbf{W}_\ell, \quad \mathbf{b}'_\ell = \mathbf{P} \mathbf{b}_\ell, \quad \mathbf{W}'_{\ell+1} = \mathbf{W}_{\ell+1} \mathbf{P}^\top$$

then the two models are functionally equivalent: $f(\mathbf{x}; \Theta) = f(\mathbf{x}; \Theta')$ for all inputs \mathbf{x} . This implies that for any trained weights Θ , there is not just one such weight assignment but an entire equivalence class of weight assignments, and your convergence to any one specific element of this equivalence class – as opposed to any of the others – is determined only by random seed. We denote a functionality-preserving permutation of weights as $\pi(\Theta)$.

Consider the task of reconciling the weights of two, independently trained models – model A and model B with weights Θ_A and Θ_B , respectively – such that we can linearly interpolate between them. We assume that models A and B were trained with equivalent architectures but different random initializations, data orders, and potentially different hyperparameters or datasets as well. Our central question is: Given Θ_A and Θ_B , can we identify some π such that when linearly interpolating between Θ_A and $\pi(\Theta_B)$, all intermediate models enjoy performance similar to Θ_A and Θ_B ?

We base any claims of loss landscape (quasi-)convexity on the usual definition of multi-dimensional convexity in terms of one-dimensional (quasi-)convexity,

Definition 2.1 (Convexity). A function $f : \mathbb{R}^D \rightarrow \mathbb{R}$ is (quasi-)convex if every one-dimensional slice is (quasi-)convex, ie. for all $x, y \in \mathbb{R}^D$, the function $g(\lambda) = f((1-\lambda)x + \lambda y)$ is (quasi-)convex in λ .

Thanks to Definition 2.1, it suffices to show that arbitrary one-dimensional slices of a function are convex in order to reason about the convexity of complex, high-dimensional functions. In practice, we rarely observe perfect convexity, but instead hope to approximate it as closely as possible. Following Draxler et al. (2018), Entezari et al. (2021), Frankle et al. (2020) and others, we measure approximations to convexity via “barriers”.

Definition 2.2 (Loss barrier (Frankle et al., 2020)). Given two points Θ_A, Θ_B such that $\mathcal{L}(\Theta_A) \approx \mathcal{L}(\Theta_B)$, the *loss barrier* is defined as $\max_{\lambda \in [0,1]} \mathcal{L}((1-\lambda)\Theta_A + \lambda\Theta_B) - \frac{1}{2}(\mathcal{L}(\Theta_A) + \mathcal{L}(\Theta_B))$.

Note that loss barriers are non-negative, with zero indicating an interpolation of flat or negative curvature.

3 Permutation selection methods

We introduce three methods of matching units between model A and model B . In addition, we present an appealing but failed method in Appendix A.2.

3.1 Matching activations

Following the classic Hebbian mantra “[neural network units] that fire together, wire together” (Hebb, 2005) we propose associating units across two models by performing regression between their activations. Matching activations between models is compelling as it captures the intuitive notion that two models must learn similar features in order to accomplish the same task (Li et al., 2016). Provided activations for each model, we wish to associate each unit in A to a unit in B . It stands to reason that there may exist a linear relationship between the activations of the two models. We fit this into the regression framework by constraining ordinary least squares (OLS) regression to solutions in the set of permutation matrices, S_d . For

¹We denote the set of all $d \times d$ permutation matrices – isomorphic to the symmetric group – as S_d , perhaps to the chagrin of pure mathematicians.

activations of the ℓ 'th layer, let $\mathbf{Z}^{(A)}, \mathbf{Z}^{(B)} \in \mathbb{R}^{d \times n}$ denote the d -dimensional activations for all n training data points, in models A and B respectively. Then,

$$\mathbf{P}_\ell = \arg \min_{\mathbf{P} \in S_d} \sum_{i=1}^n \|\mathbf{Z}_{:,i}^{(A)} - \mathbf{P} \mathbf{Z}_{:,i}^{(B)}\|^2 = \arg \min_{\mathbf{P} \in S_d} \|\mathbf{Z}^{(A)} - \mathbf{P} \mathbf{Z}^{(B)}\|_F^2 = \arg \max_{\mathbf{P} \in S_d} \langle \mathbf{P}, \mathbf{Z}^{(A)} (\mathbf{Z}^{(B)})^\top \rangle_F \quad (1)$$

where $\langle \mathbf{A}, \mathbf{B} \rangle_F = \sum_{i,j} A_{i,j} B_{i,j}$ denotes the Frobenius inner product between real-valued matrices \mathbf{A} and \mathbf{B} and $\|\mathbf{A}\|_F^2 = \langle \mathbf{A}, \mathbf{A} \rangle_F$ is the corresponding norm. Conveniently, eq. (1) constitutes a ‘‘linear assignment problem’’ problem (LAP) (Bertsekas, 1998) for which efficient, practical algorithms are known. Having solved this assignment problem on each layer, we can then permute the weights of model B to match model A as closely as possible:

$$\mathbf{W}'_\ell = \mathbf{P}_\ell \mathbf{W}_\ell^{(B)} \mathbf{P}_{\ell-1}^\top, \quad \mathbf{b}'_\ell = \mathbf{P}_\ell \mathbf{b}_\ell^{(B)}$$

for each layer ℓ , producing new weights, Θ' , such that the intermediate activations align as closely possible with those of Θ_A .

Computationally, this entire process is relatively lightweight: the $\mathbf{Z}^{(A)}$ and $\mathbf{Z}^{(B)}$ matrices can be computed in a single pass over the training dataset, and in practice, a full run through the training dataset may not even be necessary. Decent correlation estimates are likely possible with only a subset of the data. Solving eq. (1) is possible thanks to well-established, polynomial-time algorithms for solving the linear assignment problem (Kuhn, 2010; Jonker & Volgenant, 1987; Crouse, 2016). Also, conveniently, the activation matching at each layer is independent of the matching at every other layer resulting in a separable and straightforward optimization problem, an advantage that will not be enjoyed by the following methods.

Dispensing with regression, one could similarly associate units by matching against a matrix of cross-correlation coefficients in place of $\mathbf{Z}^{(A)} (\mathbf{Z}^{(B)})^\top$. We observed correlation matching to work equally well, but found matching via OLS regression to be more principled and easier to implement.

3.2 Matching weights

Instead of associating intermediate units by their activations under some data distribution, we could alternatively inspect the weights of the model itself. Consider for a moment, the first layer weights, \mathbf{W}_1 . Each row of \mathbf{W}_1 corresponds to a single feature of the model. If two such rows were equal, they would compute exactly the same feature (ignoring bias terms for the time being). And if $[\mathbf{W}_1^{(A)}]_{i,:} \approx [\mathbf{W}_1^{(B)}]_{j,:}$, it stands to reason that units i and j should be associated. Extending this idea to every layer, we are inspired to pursue the optimization,

$$\arg \min_{\pi} \|\text{vec}(\Theta_A) - \text{vec}(\pi(\Theta_B))\|^2 = \arg \max_{\pi} \text{vec}(\Theta_A) \cdot \text{vec}(\pi(\Theta_B))$$

We can re-express this in terms of the full weights,

$$\arg \max_{\pi=\{\mathbf{P}_i\}} \langle \mathbf{W}_1^{(A)}, \mathbf{P}_1 \mathbf{W}_1^{(B)} \rangle_F + \langle \mathbf{W}_2^{(A)}, \mathbf{P}_2 \mathbf{W}_2^{(B)} \mathbf{P}_1^\top \rangle_F + \dots + \langle \mathbf{W}_L^{(A)}, \mathbf{W}_L^{(B)} \mathbf{P}_{L-1}^\top \rangle_F \quad (2)$$

resulting in another matching problem. We term this formulation the ‘‘sum of bilinear assignments problem’’ (SOBLAP). Sadly, this matching problem is thornier than the classic linear assignment matching problem presented in eq. (1). Unlike the linear assignment problem of eq. (1), we are interested in permuting *both* the rows and columns of $\mathbf{W}_\ell^{(B)}$ to match $\mathbf{W}_\ell^{(A)}$, and this turns out to be crucially different from only permuting rows or only permuting columns. We formalize this difficulty as follows,

Lemma 1. *The sum of bilinear assignments problem (SOBLAP) is NP-hard – and admits no polynomial-time constant-factor approximation scheme – for $L > 2$.*

which we prove in Appendix A.3. Lemma 1 stands in stark contrast to classical LAP for which practical, polynomial-time algorithms are known.

Undeterred, we propose a greedy approximation algorithm for SOBLAP. Looking at a single \mathbf{P}_ℓ while holding the others fixed, note that the optimization problem can be reduced to a classic linear assignment problem,

$$\begin{aligned} \arg \max_{\mathbf{P}_\ell} & \langle \mathbf{W}_\ell^{(A)}, \mathbf{P}_\ell \mathbf{W}_\ell^{(B)} \mathbf{P}_{\ell-1}^\top \rangle_F + \langle \mathbf{W}_{\ell+1}^{(A)}, \mathbf{P}_{\ell+1} \mathbf{W}_{\ell+1}^{(B)} \mathbf{P}_\ell^\top \rangle_F \\ & = \arg \max_{\mathbf{P}_\ell} \langle \mathbf{P}_\ell, \mathbf{W}_\ell^{(A)} \mathbf{P}_{\ell-1} (\mathbf{W}_\ell^{(B)})^\top \rangle_F + \langle \mathbf{P}_\ell, (\mathbf{W}_{\ell+1}^{(A)})^\top \mathbf{P}_{\ell+1} \mathbf{W}_{\ell+1}^{(B)} \rangle_F \\ & = \arg \max_{\mathbf{P}_\ell} \langle \mathbf{P}_\ell, \mathbf{W}_\ell^{(A)} \mathbf{P}_{\ell-1} (\mathbf{W}_\ell^{(B)})^\top + (\mathbf{W}_{\ell+1}^{(A)})^\top \mathbf{P}_{\ell+1} \mathbf{W}_{\ell+1}^{(B)} \rangle_F \end{aligned}$$

This leads us to a convenient greedy algorithm: go through each of the layers, and greedily select the best \mathbf{P}_ℓ at that layer. Repeat until convergence. We present this in Algorithm 1.

Algorithm 1: Greedy-SOBLAP

Given: Model weights $\Theta_A = \{\mathbf{W}_1^{(A)}, \dots, \mathbf{W}_L^{(A)}\}$ and $\Theta_B = \{\mathbf{W}_1^{(B)}, \dots, \mathbf{W}_L^{(B)}\}$

Result: A permutation $\pi = \{\mathbf{P}_1, \dots, \mathbf{P}_{L-1}\}$ of Θ_B such that $\text{vec}(\Theta_A) \cdot \text{vec}(\pi(\Theta_B))$ is approximately maximized.

Initialize: $\mathbf{P}_1 \leftarrow \mathbf{I}, \dots, \mathbf{P}_{L-1} \leftarrow \mathbf{I}$

repeat

for $\ell \in \text{RandomPermutation}(1, \dots, L-1)$ **do**

$\mathbf{P}_\ell \leftarrow \text{SolveLAP} \left(\mathbf{W}_\ell^{(A)} \mathbf{P}_{\ell-1} (\mathbf{W}_\ell^{(B)})^\top + (\mathbf{W}_{\ell+1}^{(A)})^\top \mathbf{P}_{\ell+1} \mathbf{W}_{\ell+1}^{(B)} \right)$

end

until *convergence*

Although we present Algorithm 1 in terms of an MLP without bias terms, in practice our implementation can handle the weights of models of arbitrary architecture including bias terms, residual connections, convolutional layers, attention mechanisms, and so forth. In experiments we observed this algorithm to be fast in terms of both wall-clock time and iterations necessary for convergence. We did not observe any examples of it failing to converge. We defer a formal analysis of Algorithm 1 to future work.

Unlike the activation matching method presented in Section 3.1, weight matching is “blind” in the sense that it ignores the data distribution. In theory, ignoring the input data distribution and therefore the loss landscape handicaps weight matching but allows it to be much faster, running in mere seconds for all models tested. We are therefore encouraged for its potential application in fields such as fine-tuning (Devlin et al., 2019; Wortsman et al., 2022b;a), federated learning (McMahan et al., 2017; Konečný et al., 2016a;b), and model patching (Matena & Raffel, 2021; Sung et al., 2021; Raffel, 2021). In practice, we found weight matching to be surprisingly competitive with data-aware methods. A study of this trade-off is made in Section 5.

3.3 Learning permutations with a straight-through estimator

Inspired by the success of straight-through estimators (STEs) in other discrete optimization problems (Bengio et al., 2013; Kusupati et al., 2021; Rastegari et al., 2016; Courbariaux & Bengio, 2016), in this section we attempt to “learn” the ideal permutation of weights $\pi(\Theta_B)$. More specifically, our goal is to optimize

$$\min_{\tilde{\Theta}_B} \mathcal{L} \left(\frac{1}{2} (\Theta_A + \text{proj}(\tilde{\Theta}_B)) \right), \quad \text{proj}(\Theta) \triangleq \arg \max_{\pi(\Theta_B)} \text{vec}(\Theta) \cdot \text{vec}(\pi(\Theta_B)) \quad (3)$$

where $\tilde{\Theta}_B$ denotes an approximation of $\pi(\Theta_B)$, allowing us to implicitly optimize π . Tragically eq. (3) involves non-differentiable projection operations, $\text{proj}(\cdot)$, complicating the optimization. We overcome this via a “straight-through” estimator: we parameterize the problem in terms of a set of weights $\tilde{\Theta}_B \approx \pi(\Theta_B)$. In the forward pass, we project $\tilde{\Theta}_B$ to the closest realizable $\pi(\Theta_B)$. Then, in the backwards pass we switch

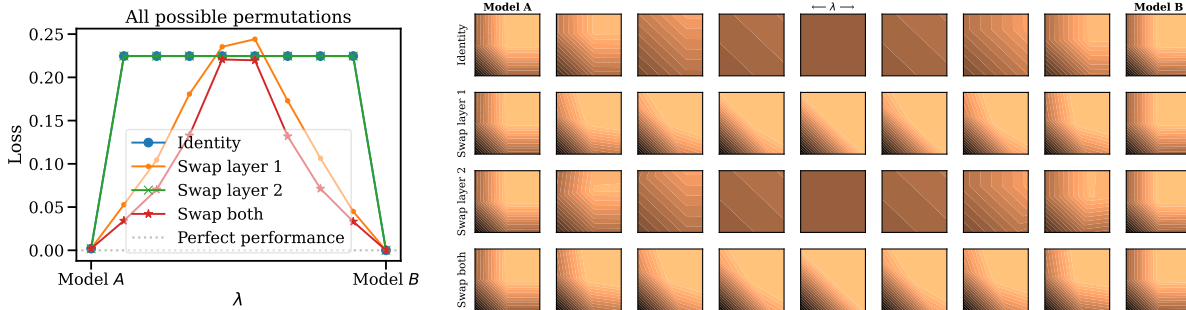


Figure 1: A counterexample: There exist models such that no possible permutation of weights allows for linear mode connectivity. *Left*: performance of all possible linear interpolations between the two models. *Right*: A visualization of the prediction functions $f(\mathbf{x})$ through each of the linear sweeps. Each row corresponds to one of the four possible permutations and each column corresponds to a value of λ , the linear interpolant. The existence of such cases suggests that linear mode connectivity is an artifact of SGD.

back to the unrestricted weights $\tilde{\Theta}_B$. In this way, we are guaranteed to stay true to the projection constraints in evaluating the loss, but are still able to get usable gradients at our current parameters, $\tilde{\Theta}_B$.²

Conveniently, we can re-purpose Algorithm 1 to solve $\text{proj}(\tilde{\Theta}_B)$. Furthermore, we found initializing $\tilde{\Theta}_B = \Theta_A$ performed better than random initialization. This is to be expected immediately at initialization since the initial matching will be equivalent to the weight matching method of Section 3.1, but it is not immediately clear why these solutions continue to outperform a random initialization asymptotically.

Algorithm 2: Straight-through estimator training

Given: Model weights Θ_A , Θ_B , and a learning rate η .

Result: A permutation π of Θ_B such that $\mathcal{L}(\frac{1}{2}(\Theta_A + \pi(\Theta_B)))$ is approximately minimized.

Initialize: $\tilde{\Theta}_B \leftarrow \Theta_A$

repeat

$\pi(\Theta_B) \leftarrow \text{proj}(\tilde{\Theta}_B)$ using Algorithm 1.

 Evaluate the loss of the midpoint, $\mathcal{L}(\frac{1}{2}(\Theta_A + \pi(\Theta_B)))$.

 Evaluate the gradient, $\nabla\mathcal{L}$, using $\tilde{\Theta}_B$ in place of $\pi(\Theta_B)$ in the backwards pass.

 Update parameters, $\tilde{\Theta}_B \leftarrow \tilde{\Theta}_B - \eta\nabla\mathcal{L}$.

until convergence

Unlike the aforementioned methods, Algorithm 2 makes an attempt to explicitly “learn” the best permutation π using a conventional training loop. By initializing to the weight matching solution of Section 3.2 and leveraging the data distribution as in Section 3.1, it seeks to offer a best-of-both-worlds solution. Sadly, this comes at a very steep computational cost relative to the other two methods.

4 Interlude: a counterexample

Before arguing for the presence of linear mode connectivity, we take a step back to consider its limitations. In this section we present a counterexample proving that there exist models that do not enjoy linear mode

²Note again that projecting according to inner product distance is equivalent to projecting according to the L_2 distance when parameterizing the estimator based on the B endpoint. We also experimented with learning the midpoint directly, $\tilde{\Theta} \approx \frac{1}{2}(\Theta_A + \pi(\Theta_B))$, in which case the L_2 and inner product projections diverge. In testing all possible variations, we found that optimizing the B endpoint had a slight advantage, but all possible variations performed admirably.

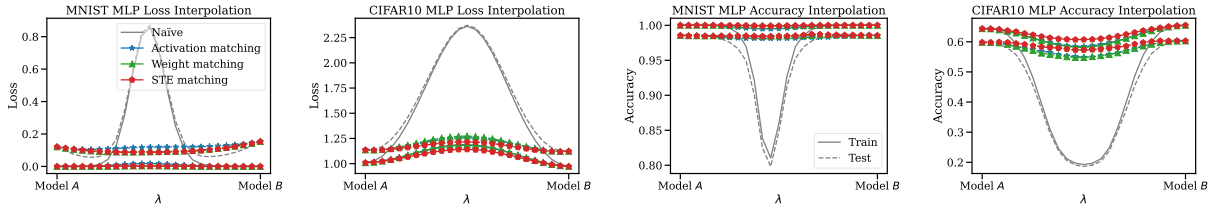


Figure 2: **Linear mode connectivity is possible after permuting.** Loss and accuracy interpolating between MLP models trained on MNIST and CIFAR-10. In all cases we are able to significantly improve over naïve interpolation. Straight-through estimator matching performs best but is very computationally expensive. Weight matching and activation matching perform similarly, even though weight matching is orders of magnitude faster and does not rely on the input data distribution.

connectivity under any permutation of weights. It follows that – to the extent we are able to achieve linear mode connectivity in practice – it is an artifact of our optimization methods, not our architectures.

Consider a simple 2-dimensional classification task: Our data points are drawn $\mathbf{x} \sim \text{Uniform}([-1, 1]^2)$ and $y = \mathbf{1}_{x_1 > 0 \text{ and } x_2 > 0}$. In other words, points in the positive quadrant are labeled $y = 1$, while everything else is labeled $y = 0$. We provide a visualization of a sample of such data in Figure 6.

We utilize an MLP architecture consisting of two hidden layers, with two units each, and ReLU nonlinearities. Consider two weight assignments that both achieve a perfect fit to the data:

$$f_A(\mathbf{x}) = [-1 \quad -1] \sigma \left(\begin{bmatrix} -1 & 0 \\ 0 & 1 \end{bmatrix} \sigma \left(\begin{bmatrix} 1 & 0 \\ 0 & -1 \end{bmatrix} \mathbf{x} + \begin{bmatrix} 1 \\ 0 \end{bmatrix} \right) + \begin{bmatrix} 1 \\ 0 \end{bmatrix} \right) \quad (4)$$

$$f_B(\mathbf{x}) = [-1 \quad -1] \sigma \left(\begin{bmatrix} 1 & 0 \\ 0 & -1 \end{bmatrix} \sigma \left(\begin{bmatrix} -1 & 0 \\ 0 & 1 \end{bmatrix} \mathbf{x} + \begin{bmatrix} 0 \\ 1 \end{bmatrix} \right) + \begin{bmatrix} 0 \\ 1 \end{bmatrix} \right) \quad (5)$$

We predict a positive label when $f(\mathbf{x}) \geq 0$ and a negative label otherwise. Intuitively, these networks are organized such that each layer makes a classification whether $\mathbf{x}_1 > 0$ or $\mathbf{x}_2 > 0$. In model A , the first layer tests whether $\mathbf{x}_2 > 0$ and the second layer tests whether $\mathbf{x}_1 > 0$, whereas in model B the order is reversed. With a bit of algebra, it is possible to see that both f_A and f_B achieve perfect performance.

Since these networks have small width, we can simply inspect all four possible permutations of the intermediate units. We visualize this in Figure 1. Critically, no permutation results in linear mode connectivity.

We present this counterexample in part to establish some basic intuition for Conjecture 1, but more importantly to highlight that any success interpolating between permuted networks is due to inherent bias in the optimization algorithms used and not the network architectures themselves. We have SGD to thank any time we find two independent models that admit some form of linear mode connectivity. We also take this opportunity to point out that there are invariances beyond permutation symmetries: It is also possible to move features between layers, re-scale layers, and so forth. Prior works have previously pointed out the feature/layer-association (Nguyen et al., 2021) and layer re-scaling invariances (Ainsworth et al., 2018), albeit in different contexts.

5 Experiments

Our base experimental methodology will be to separately train two models, A and B , starting from different random initializations and with different random batch orders, resulting in trained weights Θ_A and Θ_B respectively. We then evaluate slices through the loss landscape, $\mathcal{L}((1-\lambda)\Theta_A + \lambda\pi(\Theta_B))$ for $\lambda \in [0, 1]$, where π is selected according to the methods presented in Section 3.³ Ideally, we seek a completely flat or even convex

³We also experimented with spherical linear interpolation (“slerp”) and found that it performed slightly better than linear interpolation but that the difference was not significant enough to warrant diverging from the pre-existing literature.

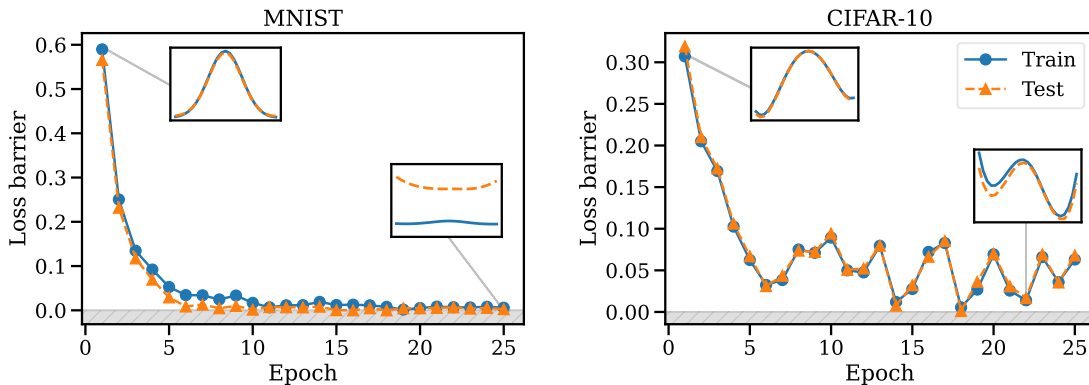


Figure 3: **Linear mode connectivity does not work at initialization.** Loss barriers as a function of training time for MLPs trained on MNIST (left) and CIFAR-10 (right). Loss interpolation plots inlaid to highlight results in initial and later epochs. LMC manifests gradually as models are trained. The single basin theory does not hold for models at initialization, suggesting distinct loss landscape geometries at the beginning and end phases of training. We hypothesize that the variance in CIFAR-10 training is higher due to our MLP architecture being under-powered relative to the dataset. (The y-axis scales differ in each of the inlaid plots.)

one-dimensional slice. As discussed in Section 2, the ability to exhibit this behavior for arbitrary Θ_A, Θ_B empirically suggests that the loss landscape contains only a single basin modulo permutation symmetries.

We remark that a failure to find a π such that linear mode connectivity holds cannot rule out the existence of a satisfactory permutation. Given the astronomical number of permutation symmetries, Conjecture 1 is essentially impossible to disprove for any realistically wide model architecture.

5.1 Loss landscapes before and after matching

We present results for MLPs trained on MNIST (LeCun et al., 1998) and CIFAR-10 (Krizhevsky, 2009) in Figure 2. Naïve interpolation ($\pi(\Theta) = \Theta$) results in substantial performance degradation when interpolating. On the other hand, the methods introduced in Section 3 are able to achieve much better barriers. We achieve zero-barrier linear mode connectivity on MNIST with all three methods, although activation matching performs just slightly less favorably than weight matching and straight-through estimator (STE) matching. We especially note that the test loss landscape is made convex after applying our weight matching and STE permutations! In other words, our interpolation actually yields a merged model that outperforms both model A and B . We expand on this phenomenon in Section 5.4.

On CIFAR-10 we fall short of zero-barrier connections between MLP solutions, although we do see a ten-fold decrease in barrier relative to naïve interpolation. On CIFAR-10 the benefits of STE relative to weight matching become more clear. We see that STE matching identifies a noticeably better permutation than the other two methods. CIFAR-10 is not out-of-reach, however. As we demonstrate in Section 5.3, we are able to achieve zero-barrier LMC on CIFAR-10 with large ResNet models. Therefore, we hypothesize that the presence of linear mode connectivity is dependent on the capacity of the model being sufficient to capture the complexity of the input data distribution.

STE matching, the most expensive method, produces the best solutions as expected. Somewhat surprising however is that the gap between STE and the other two methods is not all that large. In particular, it is remarkable how much can be done without looking at the input data at all! We found that weight matching offered a very compelling balance between computational cost and performance: it runs in mere seconds (on modern hardware at the time of writing), and produces high quality solutions. On the other hand, activation

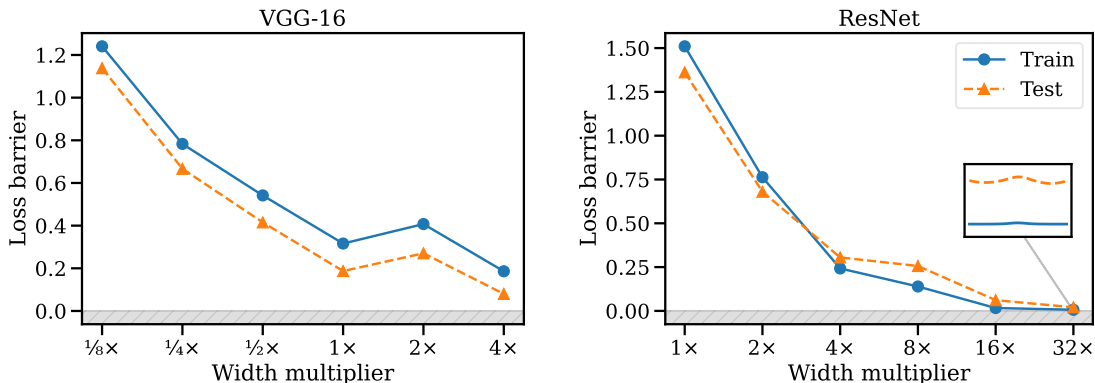


Figure 4: **Wider models exhibit better linear mode connectivity.** Training convolutional and ResNet architectures on CIFAR-10, we ablate their width and visualize their loss barriers after weight matching. Notably, we achieve zero-barrier LMC between ResNet models, the first such demonstration to the best of the authors’ knowledge.

matching appears to be of little utility as it is more expensive to run and did not produce higher quality solutions in our experiments.

5.2 Onset of mode connectivity

Given the results of Section 5.1 it may be tempting to conclude that the entirety of weight space contains only a single basin modulo permutation symmetries. However we found that linear mode connectivity is an emergent property of SGD training, and we were unable to uncover it early in training. We explore the emergence of linear mode connectivity in Figure 3. The emergence of LMC partway through training fits with previous works suggesting that training consists of an initial “burn-in” phase followed by a much longer “tuning” phase (Frankle et al., 2020).

Note also that the final inlaid interpolation plot in Figure 3(right) demonstrates an important shortcoming of the loss barrier metric: the interpolation includes points with lower loss than either of the two models, however the loss barrier is still positive due to non-negativity as mentioned in Section 2.

5.3 Effect of model width

Conventional wisdom suggests that wider architectures are easier to optimize (Jacot et al., 2018; Lee et al., 2019). In this section, we investigate whether wider architectures are also easier to linearly mode connect. We train VGG-16 (Simonyan & Zisserman, 2015) and ResNet20 (He et al., 2016) architectures of varying width on the CIFAR-10 dataset. Results are presented in Figure 4. Sadly, 8x width VGG-16 training was unattainable as it exhausted GPU memory on available hardware at the time of writing.

As expected, there is a clear relationship between model width and linear mode connectivity, as measured by the loss barrier between solutions. Although 1x-sized models did not seem to exhibit linear mode connectivity, we found that larger width models decreased loss barriers all the way to zero. In Figure 4(right) we show the first ever demonstration – to the best of the authors’ knowledge – of zero-barrier linear mode connectivity between two large ResNet models trained on a non-trivial dataset.

It is essential to point out that relatively skinny models do not seem to obey linear mode connectivity, yet still exhibit similarities in training dynamics. This suggests that either our permutation selection methods are failing to find satisfactory permutations on skinnier models or that some form of invariance other than permutation symmetries must be at play in the skinny model regime.

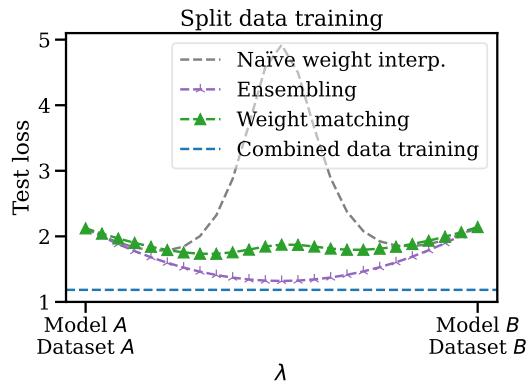


Figure 5: **Models trained on disjoint datasets can be merged with positive-sum results.** Two ResNet models trained on disjoint, biased subsets of CIFAR-100 can be merged in weight space, thanks to Algorithm 1.

5.4 Model patching and split data training

Inspired by work on fine-tuning (Wortsman et al., 2022a), model patching (Raffel, 2021), and federated learning (McMahan et al., 2017; Konečný et al., 2016a;b), we study whether it is possible to synergistically merge the weights of two models trained on disjoint datasets. Consider for example an organization with multiple (possibly biased!) datasets separated for regulatory (eg. GDPR) or privacy (eg. on-device data) considerations. Models can be trained on each dataset individually but training in aggregate is not feasible. Can we combine separately trained models in such a way that the merged model outperforms the input models on the entirety of the data?

To address this question we split the CIFAR-100 dataset (Krizhevsky, 2009) into two disjoint subsets: dataset A , containing 20% examples labelled 0-49 and 80% labelled 50-99, and dataset B vice-versa. No image exists in both dataset A and B . ResNet20 models A and B were trained on their corresponding datasets. We show the result of merging the two models with weight matching in Figure 5. Naïve weight interpolation, ensembling of the model logits, and full-data training are also benchmarked for comparison.

As expected, merging separately-trained models with weight matching was not able to match the performance of omniscient model trained on the full dataset, or an ensemble of the two models with twice the number of effective weights. On the other hand, we did manage to merge the two models in weight space achieving an interpolated model that outperforms both input models in terms of test loss while using half the memory and compute required for ensembling. It also vastly outperformed naïve interpolation, the status quo for model combination in federated learning. Incorporating Algorithm 1 into a federated learning framework could be an exciting avenue for future work.

6 Related work

(Linear) mode connectivity Garipov et al. (2018) introduced the concept of mode connectivity: the idea that SGD solutions in the loss landscape are connected by constant-loss curves in weight space. Further explorations were undertaken in Freeman & Bruna (2017); Draxler et al. (2018) among others. Frankle et al. (2020) demonstrated a connection between *linear* mode connectivity and the lottery ticket hypothesis. Brea et al. (2019) noted the existence of permutation symmetries and implicated them as a source of saddle points in the loss landscape. Recently, Entezari et al. (2021) conjectured that SGD solutions could be linear mode connected modulo permutation symmetries.

Loss landscapes and training dynamics Li et al. (2016); Yosinski et al. (2014) investigated whether independently trained networks learn similar features, and to what extent they transfer. Jiang et al. (2021)

argued that independently trained networks meaningfully differ in the features they learn in certain scenarios. Zhang et al. (2019) studied the relative importance of layers and the features they learn. Li et al. (2018) showed that residual connections result in smoother loss landscapes. On the theoretical front, Kawaguchi (2016) proved that deep linear networks contain no local minima. In other words, every local minima is a global minima. Boursier et al. (2022) characterized the training dynamics of one-hidden layer ReLU networks on orthogonal data, including a proof that they converge to zero loss.

Federated learning and model merging McMahan et al. (2017); Konečný et al. (2016a;b) introduced the concept of “federated learning”: learning split across multiple devices and data. Wang et al. (2020) proposed an exciting federated learning method in which model averaging is done after permuting units. Unlike this work, however, they proposed merging smaller “child” models into a larger “main” model, and doing so with a more specific, layer-wise matching algorithm that does not support residual connections or normalization layers. Raffel (2021); Matena & Raffel (2021); Sung et al. (2021) conceptualized the study of “model patching”, the idea that models should be easy to modify and submit changes to. Singh & Jaggi (2020) proposed merging models by soft-aligning associations weights, inspired by optimal transport. Wortsman et al. (2022a) demonstrated state-of-the-art ImageNet performance by averaging weights of models fine-tuned starting from some initial trained state.

Differentiating through permutations Akin to differentiable permutation learning, a number of prior works have studied differentiable sorting (Grover et al., 2019; Prillo & Eisenschlos, 2020; Cuturi et al., 2019; Petersen et al., 2022; 2021; Mena et al., 2018). Blondel et al. (2020) studied differentiable sorting and ranking with asymptotics that correspond to their non-differentiable versions. Fogel et al. (2015) explored recovering the linear orderings of items based on pairwise information, another form of permutation optimization. Bengio et al. (2013) introduced the straight-through estimator for differentiating through discrete projections that we utilize in Section 3.3.

7 Discussion and future work

We explore the role of permutation symmetries in the linear mode connectivity of SGD solutions in deep learning. We introduce three novel algorithms, of varying complexity and computational cost, to canonicalize independent neural network weights such that the loss landscape between them is made as flat as possible. In contrast to prior work, we are able to linearly mode connect large ResNet models in mere seconds. Despite presenting successes across multiple architectures and datasets, linear mode connectivity between thin models remains elusive even though thin models also exhibit phenomenon suggesting some underlying invariances in their training dynamics. Therefore we conjecture that the permutation symmetry hypothesis is a necessary piece, though not a complete picture, of whatever fundamental invariances are at play in neural network training dynamics. In particular, we hypothesize that SGD is biased towards solutions such that there is a linear relationship between layer-wise activations across models. In the infinite width limit it just so happens that there exist satisfactory linear relationships that are also a permutations.

An expanded theory and empirical exploration of other invariances – such as cross-layer scaling or general linear relationships between activations – would be an exciting avenue for future work. Ultimately, it is our hope that a lucid understanding of loss landscape geometry will not only advance the theory of deep learning but will also unlock the development of better optimization, federated learning, and ensembling techniques.

Broader Impact Statement

Merging models raises interesting ethical and technical questions about the resulting models. Do they contain the same biases as their input models? Are some rare examples forgotten when merging? Is it possible to gerrymander a subset of the dataset by splitting its elements across many shards?

Deployment of any form of model merging ought to be paired with thorough auditing of the resulting model, and in particular whether it is representative of the entirety of the data distribution.

Acknowledgments

Thank you to Mitchell Wortsman, Aditya Kusupati, Rahim Entezari, Jason Yosinski, Krishna Pillutla, Ofir Press, Matt Wallingford, Vivek Ramanujan, Tim Dettmers, Kevin Jamieson, and Sewoong Oh for enlightening discussions. Thank you to John Thickstun for his thoughtful review of an earlier draft of this work. This work was (partially) funded by the National Science Foundation NRI (#2132848) & CHS (#2007011), DARPA RACER, the Office of Naval Research, Honda Research Institute, and Amazon.

References

- Samuel K. Ainsworth, Nicholas J. Foti, Adrian K. C. Lee, and Emily B. Fox. oi-vae: Output interpretable vae for nonlinear group factor analysis. In Jennifer G. Dy and Andreas Krause (eds.), *Proceedings of the 35th International Conference on Machine Learning, ICML 2018, Stockholm, Sweden, July 10-15, 2018*, volume 80 of *Proceedings of Machine Learning Research*, pp. 119–128. PMLR, 2018. URL <http://proceedings.mlr.press/v80/ainsworth18a.html>.
- Samuel K. Ainsworth, Kendall Lowrey, John Thickstun, Zaïd Harchaoui, and Siddhartha S. Srinivasa. Faster policy learning with continuous-time gradients. In Ali Jadbabaie, John Lygeros, George J. Pappas, Pablo A. Parrilo, Benjamin Recht, Claire J. Tomlin, and Melanie N. Zeilinger (eds.), *Proceedings of the 3rd Annual Conference on Learning for Dynamics and Control, L4DC 2021, 7-8 June 2021, Virtual Event, Switzerland*, volume 144 of *Proceedings of Machine Learning Research*, pp. 1054–1067. PMLR, 2021. URL <http://proceedings.mlr.press/v144/ainsworth21a.html>.
- Yoshua Bengio, Nicholas Léonard, and Aaron C. Courville. Estimating or propagating gradients through stochastic neurons for conditional computation. *CoRR*, abs/1308.3432, 2013. URL <http://arxiv.org/abs/1308.3432>.
- D.P. Bertsekas. *Network Optimization: Continuous and Discrete Methods*. Athena scientific optimization and computation series. Athena Scientific, 1998. ISBN 9788865290279. URL <https://books.google.com/books?id=afYYAQAAIAAJ>.
- Christopher M. Bishop. *Pattern recognition and machine learning, 5th Edition*. Information science and statistics. Springer, 2007. ISBN 9780387310732. URL <https://www.worldcat.org/oclc/71008143>.
- Mathieu Blondel, Olivier Teboul, Quentin Berthet, and Josip Djolonga. Fast differentiable sorting and ranking. In *Proceedings of the 37th International Conference on Machine Learning, ICML 2020, 13-18 July 2020, Virtual Event*, volume 119 of *Proceedings of Machine Learning Research*, pp. 950–959. PMLR, 2020. URL <http://proceedings.mlr.press/v119/blondel20a.html>.
- Etienne Boursier, Loucas Pillaud-Vivien, and Nicolas Flammarion. Gradient flow dynamics of shallow relu networks for square loss and orthogonal inputs. *CoRR*, abs/2206.00939, 2022. doi: 10.48550/arXiv.2206.00939. URL <https://doi.org/10.48550/arXiv.2206.00939>.
- Johanni Brea, Berfin Simsek, Bernd Illing, and Wulfram Gerstner. Weight-space symmetry in deep networks gives rise to permutation saddles, connected by equal-loss valleys across the loss landscape. *CoRR*, abs/1907.02911, 2019. URL <http://arxiv.org/abs/1907.02911>.
- E. Cela. *The Quadratic Assignment Problem: Theory and Algorithms*. Combinatorial Optimization. Springer US, 2013. ISBN 9781475727876. URL <https://books.google.com/books?id=20QGCAAQBAJ>.
- Matthieu Courbariaux and Yoshua Bengio. Binarynet: Training deep neural networks with weights and activations constrained to +1 or -1. *CoRR*, abs/1602.02830, 2016. URL <http://arxiv.org/abs/1602.02830>.
- David Frederic Crouse. On implementing 2d rectangular assignment algorithms. *IEEE Trans. Aerosp. Electron. Syst.*, 52(4):1679–1696, 2016. doi: 10.1109/TAES.2016.140952. URL <https://doi.org/10.1109/TAES.2016.140952>.
- Marco Cuturi, Olivier Teboul, and Jean-Philippe Vert. Differentiable ranks and sorting using optimal transport. *CoRR*, abs/1905.11885, 2019. URL <http://arxiv.org/abs/1905.11885>.
- Jacob Devlin, Ming-Wei Chang, Kenton Lee, and Kristina Toutanova. BERT: pre-training of deep bidirectional transformers for language understanding. In Jill Burstein, Christy Doran, and Thamar Solorio (eds.), *Proceedings of the 2019 Conference of the North American Chapter of the Association for Computational Linguistics: Human Language Technologies, NAACL-HLT 2019, Minneapolis, MN, USA, June 2-7, 2019, Volume 1 (Long and Short Papers)*, pp. 4171–4186. Association for Computational Linguistics, 2019. doi: 10.18653/v1/n19-1423. URL <https://doi.org/10.18653/v1/n19-1423>.

-
- Felix Draxler, Kambis Veschgini, Manfred Salmhofer, and Fred A. Hamprecht. Essentially no barriers in neural network energy landscape. In Jennifer G. Dy and Andreas Krause (eds.), *Proceedings of the 35th International Conference on Machine Learning, ICML 2018, Stockholmsmässan, Stockholm, Sweden, July 10-15, 2018*, volume 80 of *Proceedings of Machine Learning Research*, pp. 1308–1317. PMLR, 2018. URL <http://proceedings.mlr.press/v80/draxler18a.html>.
- Rahim Entezari, Hanie Sedghi, Olga Saukh, and Behnam Neyshabur. The role of permutation invariance in linear mode connectivity of neural networks. *CoRR*, abs/2110.06296, 2021. URL <https://arxiv.org/abs/2110.06296>.
- Fajwel Fogel, Rodolphe Jenatton, Francis R. Bach, and Alexandre d’Aspremont. Convex relaxations for permutation problems. *SIAM J. Matrix Anal. Appl.*, 36(4):1465–1488, 2015. doi: 10.1137/130947362. URL <https://doi.org/10.1137/130947362>.
- Jonathan Frankle. Revisiting "qualitatively characterizing neural network optimization problems". *CoRR*, abs/2012.06898, 2020. URL <https://arxiv.org/abs/2012.06898>.
- Jonathan Frankle, Gintare Karolina Dziugaite, Daniel M. Roy, and Michael Carbin. Linear mode connectivity and the lottery ticket hypothesis. In *Proceedings of the 37th International Conference on Machine Learning, ICML 2020, 13-18 July 2020, Virtual Event*, volume 119 of *Proceedings of Machine Learning Research*, pp. 3259–3269. PMLR, 2020. URL <http://proceedings.mlr.press/v119/frankle20a.html>.
- C. Daniel Freeman and Joan Bruna. Topology and geometry of half-rectified network optimization. In *5th International Conference on Learning Representations, ICLR 2017, Toulon, France, April 24-26, 2017, Conference Track Proceedings*. OpenReview.net, 2017. URL <https://openreview.net/forum?id=Bk0FWvcgx>.
- Timur Garipov, Pavel Izmailov, Dmitrii Podoprikin, Dmitry P. Vetrov, and Andrew Gordon Wilson. Loss surfaces, mode connectivity, and fast ensembling of dnns. In Samy Bengio, Hanna M. Wallach, Hugo Larochelle, Kristen Grauman, Nicolò Cesa-Bianchi, and Roman Garnett (eds.), *Advances in Neural Information Processing Systems 31: Annual Conference on Neural Information Processing Systems 2018, NeurIPS 2018, December 3-8, 2018, Montréal, Canada*, pp. 8803–8812, 2018. URL <https://proceedings.neurips.cc/paper/2018/hash/be3087e74e9100d4bc4c6268cdbe8456-Abstract.html>.
- Ian J. Goodfellow and Oriol Vinyals. Qualitatively characterizing neural network optimization problems. In Yoshua Bengio and Yann LeCun (eds.), *3rd International Conference on Learning Representations, ICLR 2015, San Diego, CA, USA, May 7-9, 2015, Conference Track Proceedings*, 2015. URL <http://arxiv.org/abs/1412.6544>.
- Aditya Grover, Eric Wang, Aaron Zweig, and Stefano Ermon. Stochastic optimization of sorting networks via continuous relaxations. In *7th International Conference on Learning Representations, ICLR 2019, New Orleans, LA, USA, May 6-9, 2019*. OpenReview.net, 2019. URL <https://openreview.net/forum?id=H1eSS3CkKX>.
- Kaiming He, Xiangyu Zhang, Shaoqing Ren, and Jian Sun. Deep residual learning for image recognition. In *2016 IEEE Conference on Computer Vision and Pattern Recognition, CVPR 2016, Las Vegas, NV, USA, June 27-30, 2016*, pp. 770–778. IEEE Computer Society, 2016. doi: 10.1109/CVPR.2016.90. URL <https://doi.org/10.1109/CVPR.2016.90>.
- Donald Olding Hebb. *The organization of behavior: A neuropsychological theory*. Psychology Press, 2005.
- Arthur Jacot, Clément Hongler, and Franck Gabriel. Neural tangent kernel: Convergence and generalization in neural networks. In Samy Bengio, Hanna M. Wallach, Hugo Larochelle, Kristen Grauman, Nicolò Cesa-Bianchi, and Roman Garnett (eds.), *Advances in Neural Information Processing Systems 31: Annual Conference on Neural Information Processing Systems 2018, NeurIPS 2018, December 3-8, 2018, Montréal, Canada*, pp. 8580–8589, 2018. URL <https://proceedings.neurips.cc/paper/2018/hash/5a4be1fa34e62bb8a6ec6b91d2462f5a-Abstract.html>.
- Yiding Jiang, Vaishnavh Nagarajan, Christina Baek, and J. Zico Kolter. Assessing generalization of SGD via disagreement. *CoRR*, abs/2106.13799, 2021. URL <https://arxiv.org/abs/2106.13799>.

-
- Roy Jonker and A. Volgenant. A shortest augmenting path algorithm for dense and sparse linear assignment problems. *Computing*, 38(4):325–340, 1987. doi: 10.1007/BF02278710. URL <https://doi.org/10.1007/BF02278710>.
- Zhao Kang, Chong Peng, and Qiang Cheng. Top-n recommender system via matrix completion. In Dale Schuurmans and Michael P. Wellman (eds.), *Proceedings of the Thirtieth AAAI Conference on Artificial Intelligence, February 12-17, 2016, Phoenix, Arizona, USA*, pp. 179–185. AAAI Press, 2016. URL <http://www.aaai.org/ocs/index.php/AAAI/AAAI16/paper/view/11824>.
- Kenji Kawaguchi. Deep learning without poor local minima. In Daniel D. Lee, Masashi Sugiyama, Ulrike von Luxburg, Isabelle Guyon, and Roman Garnett (eds.), *Advances in Neural Information Processing Systems 29: Annual Conference on Neural Information Processing Systems 2016, December 5-10, 2016, Barcelona, Spain*, pp. 586–594, 2016. URL <https://proceedings.neurips.cc/paper/2016/hash/f2fc990265c712c49d51a18a32b39f0c-Abstract.html>.
- Matthew Kelly. An introduction to trajectory optimization: How to do your own direct collocation. *SIAM Rev.*, 59(4):849–904, 2017. doi: 10.1137/16M1062569. URL <https://doi.org/10.1137/16M1062569>.
- Jakub Konečný, H. Brendan McMahan, Daniel Ramage, and Peter Richtárik. Federated optimization: Distributed machine learning for on-device intelligence. *CoRR*, abs/1610.02527, 2016a. URL <http://arxiv.org/abs/1610.02527>.
- Jakub Konečný, H. Brendan McMahan, Felix X. Yu, Peter Richtárik, Ananda Theertha Suresh, and Dave Bacon. Federated learning: Strategies for improving communication efficiency. *CoRR*, abs/1610.05492, 2016b. URL <http://arxiv.org/abs/1610.05492>.
- Tjalling C. Koopmans and Martin Beckmann. Assignment problems and the location of economic activities. *Econometrica*, 25(1):53–76, 1957. ISSN 00129682, 14680262. URL <http://www.jstor.org/stable/1907742>.
- Alex Krizhevsky. Learning multiple layers of features from tiny images. Technical report, 2009.
- Harold W. Kuhn. The hungarian method for the assignment problem. In Michael Jünger, Thomas M. Lieblich, Denis Naddef, George L. Nemhauser, William R. Pulleyblank, Gerhard Reinelt, Giovanni Rinaldi, and Laurence A. Wolsey (eds.), *50 Years of Integer Programming 1958-2008 - From the Early Years to the State-of-the-Art*, pp. 29–47. Springer, 2010. doi: 10.1007/978-3-540-68279-0_2. URL https://doi.org/10.1007/978-3-540-68279-0_2.
- Aditya Kusupati, Matthew Wallingford, Vivek Ramanujan, Raghav Somani, Jae Sung Park, Krishna P. L. Prateek Jain, Sham M. Kakade, and Ali Farhadi. LLC: accurate, multi-purpose learnt low-dimensional binary codes. In Marc’Aurelio Ranzato, Alina Beygelzimer, Yann N. Dauphin, Percy Liang, and Jennifer Wortman Vaughan (eds.), *Advances in Neural Information Processing Systems 34: Annual Conference on Neural Information Processing Systems 2021, NeurIPS 2021, December 6-14, 2021, virtual*, pp. 23900–23913, 2021. URL <https://proceedings.neurips.cc/paper/2021/hash/c88d8d0a6097754525e02c2246d8d27f-Abstract.html>.
- Yann LeCun, Léon Bottou, Yoshua Bengio, and Patrick Haffner. Gradient-based learning applied to document recognition. *Proc. IEEE*, 86(11):2278–2324, 1998. doi: 10.1109/5.726791. URL <https://doi.org/10.1109/5.726791>.
- Jaehoon Lee, Lechao Xiao, Samuel S. Schoenholz, Yasaman Bahri, Roman Novak, Jascha Sohl-Dickstein, and Jeffrey Pennington. Wide neural networks of any depth evolve as linear models under gradient descent. In Hanna M. Wallach, Hugo Larochelle, Alina Beygelzimer, Florence d’Alché-Buc, Emily B. Fox, and Roman Garnett (eds.), *Advances in Neural Information Processing Systems 32: Annual Conference on Neural Information Processing Systems 2019, NeurIPS 2019, December 8-14, 2019, Vancouver, BC, Canada*, pp. 8570–8581, 2019. URL <https://proceedings.neurips.cc/paper/2019/hash/0d1a9651497a38d8b1c3871c84528bd4-Abstract.html>.

-
- Hao Li, Zheng Xu, Gavin Taylor, Christoph Studer, and Tom Goldstein. Visualizing the loss landscape of neural nets. In Samy Bengio, Hanna M. Wallach, Hugo Larochelle, Kristen Grauman, Nicolò Cesa-Bianchi, and Roman Garnett (eds.), *Advances in Neural Information Processing Systems 31: Annual Conference on Neural Information Processing Systems 2018, NeurIPS 2018, December 3-8, 2018, Montréal, Canada*, pp. 6391–6401, 2018. URL <https://proceedings.neurips.cc/paper/2018/hash/a41b3bb3e6b050b6c9067c67f663b915-Abstract.html>.
- Yixuan Li, Jason Yosinski, Jeff Clune, Hod Lipson, and John E. Hopcroft. Convergent learning: Do different neural networks learn the same representations? In Yoshua Bengio and Yann LeCun (eds.), *4th International Conference on Learning Representations, ICLR 2016, San Juan, Puerto Rico, May 2-4, 2016, Conference Track Proceedings*, 2016. URL <http://arxiv.org/abs/1511.07543>.
- James Lucas, Juhan Bae, Michael R. Zhang, Stanislav Fort, Richard S. Zemel, and Roger B. Grosse. On monotonic linear interpolation of neural network parameters. In Marina Meila and Tong Zhang (eds.), *Proceedings of the 38th International Conference on Machine Learning, ICML 2021, 18-24 July 2021, Virtual Event*, volume 139 of *Proceedings of Machine Learning Research*, pp. 7168–7179. PMLR, 2021. URL <http://proceedings.mlr.press/v139/lucas21a.html>.
- Konstantin Makarychev, Rajsekar Manokaran, and Maxim Sviridenko. Maximum quadratic assignment problem: Reduction from maximum label cover and lp-based approximation algorithm. *ACM Trans. Algorithms*, 10(4):18:1–18:18, 2014. doi: 10.1145/2629672. URL <https://doi.org/10.1145/2629672>.
- Michael Matena and Colin Raffel. Merging models with fisher-weighted averaging. *CoRR*, abs/2111.09832, 2021. URL <https://arxiv.org/abs/2111.09832>.
- Brendan McMahan, Eider Moore, Daniel Ramage, Seth Hampson, and Blaise Agüera y Arcas. Communication-efficient learning of deep networks from decentralized data. In Aarti Singh and Xiaojin (Jerry) Zhu (eds.), *Proceedings of the 20th International Conference on Artificial Intelligence and Statistics, AISTATS 2017, 20-22 April 2017, Fort Lauderdale, FL, USA*, volume 54 of *Proceedings of Machine Learning Research*, pp. 1273–1282. PMLR, 2017. URL <http://proceedings.mlr.press/v54/mcmahan17a.html>.
- Gonzalo E. Mena, David Belanger, Scott W. Linderman, and Jasper Snoek. Learning latent permutations with gumbel-sinkhorn networks. In *6th International Conference on Learning Representations, ICLR 2018, Vancouver, BC, Canada, April 30 - May 3, 2018, Conference Track Proceedings*. OpenReview.net, 2018. URL <https://openreview.net/forum?id=Byt3oJ-0W>.
- Thao Nguyen, Maithra Raghu, and Simon Kornblith. Do wide and deep networks learn the same things? uncovering how neural network representations vary with width and depth. In *9th International Conference on Learning Representations, ICLR 2021, Virtual Event, Austria, May 3-7, 2021*. OpenReview.net, 2021. URL <https://openreview.net/forum?id=KJNcAkY8tY4>.
- Felix Petersen, Christian Borgelt, Hilde Kuehne, and Oliver Deussen. Differentiable sorting networks for scalable sorting and ranking supervision. *CoRR*, abs/2105.04019, 2021. URL <https://arxiv.org/abs/2105.04019>.
- Felix Petersen, Christian Borgelt, Hilde Kuehne, and Oliver Deussen. Monotonic differentiable sorting networks. *CoRR*, abs/2203.09630, 2022. doi: 10.48550/arXiv.2203.09630. URL <https://doi.org/10.48550/arXiv.2203.09630>.
- Sebastian Prillo and Julian Eisenschlos. Softsort: A continuous relaxation for the argsort operator. In *Proceedings of the 37th International Conference on Machine Learning, ICML 2020, 13-18 July 2020, Virtual Event*, volume 119 of *Proceedings of Machine Learning Research*, pp. 7793–7802. PMLR, 2020. URL <http://proceedings.mlr.press/v119/prillo20a.html>.
- Colin Raffel. A call to build models like we build open-source software. <https://colinraffel.com/blog/a-call-to-build-models-like-we-build-open-source-software.html>, 2021. Accessed: 2022-06-17.

-
- Mohammad Rastegari, Vicente Ordonez, Joseph Redmon, and Ali Farhadi. Xnor-net: Imagenet classification using binary convolutional neural networks. In Bastian Leibe, Jiri Matas, Nicu Sebe, and Max Welling (eds.), *Computer Vision - ECCV 2016 - 14th European Conference, Amsterdam, The Netherlands, October 11-14, 2016, Proceedings, Part IV*, volume 9908 of *Lecture Notes in Computer Science*, pp. 525–542. Springer, 2016. doi: 10.1007/978-3-319-46493-0_32. URL https://doi.org/10.1007/978-3-319-46493-0_32.
- Sartaj Sahni and Teofilo F. Gonzalez. P-complete approximation problems. *J. ACM*, 23(3):555–565, 1976. doi: 10.1145/321958.321975. URL <https://doi.org/10.1145/321958.321975>.
- Karen Simonyan and Andrew Zisserman. Very deep convolutional networks for large-scale image recognition. In Yoshua Bengio and Yann LeCun (eds.), *3rd International Conference on Learning Representations, ICLR 2015, San Diego, CA, USA, May 7-9, 2015, Conference Track Proceedings*, 2015. URL <http://arxiv.org/abs/1409.1556>.
- Sidak Pal Singh and Martin Jaggi. Model fusion via optimal transport. In Hugo Larochelle, Marc’Aurelio Ranzato, Raia Hadsell, Maria-Florina Balcan, and Hsuan-Tien Lin (eds.), *Advances in Neural Information Processing Systems 33: Annual Conference on Neural Information Processing Systems 2020, NeurIPS 2020, December 6-12, 2020, virtual*, 2020. URL <https://proceedings.neurips.cc/paper/2020/hash/fb2697869f56484404c8ceee2985b01d-Abstract.html>.
- Yi-Lin Sung, Varun Nair, and Colin Raffel. Training neural networks with fixed sparse masks. In Marc’Aurelio Ranzato, Alina Beygelzimer, Yann N. Dauphin, Percy Liang, and Jennifer Wortman Vaughan (eds.), *Advances in Neural Information Processing Systems 34: Annual Conference on Neural Information Processing Systems 2021, NeurIPS 2021, December 6-14, 2021, virtual*, pp. 24193–24205, 2021. URL <https://proceedings.neurips.cc/paper/2021/hash/cb2653f548f8709598e8b5156738cc51-Abstract.html>.
- Tiffany Vlaar and Jonathan Frankle. What can linear interpolation of neural network loss landscapes tell us? *CoRR*, abs/2106.16004, 2021. URL <https://arxiv.org/abs/2106.16004>.
- Hongyi Wang, Mikhail Yurochkin, Yuekai Sun, Dimitris S. Papailiopoulos, and Yasaman Khazaeni. Federated learning with matched averaging. In *8th International Conference on Learning Representations, ICLR 2020, Addis Ababa, Ethiopia, April 26-30, 2020*. OpenReview.net, 2020. URL <https://openreview.net/forum?id=BkluqlSFDS>.
- Mitchell Wortsman, Gabriel Ilharco, Samir Yitzhak Gadre, Rebecca Roelofs, Raphael Gontijo-Lopes, Ari S Morcos, Hongseok Namkoong, Ali Farhadi, Yair Carmon, Simon Kornblith, et al. Model soups: averaging weights of multiple fine-tuned models improves accuracy without increasing inference time. *Proceedings of the 39th International Conference on Machine Learning, ICML 2022*, 2022a.
- Mitchell Wortsman, Gabriel Ilharco, Jong Wook Kim, Mike Li, Simon Kornblith, Rebecca Roelofs, Raphael Gontijo Lopes, Hannaneh Hajishirzi, Ali Farhadi, Hongseok Namkoong, et al. Robust fine-tuning of zero-shot models. In *Proceedings of the IEEE/CVF Conference on Computer Vision and Pattern Recognition*, pp. 7959–7971, 2022b.
- Jason Yosinski, Jeff Clune, Yoshua Bengio, and Hod Lipson. How transferable are features in deep neural networks? In Zoubin Ghahramani, Max Welling, Corinna Cortes, Neil D. Lawrence, and Kilian Q. Weinberger (eds.), *Advances in Neural Information Processing Systems 27: Annual Conference on Neural Information Processing Systems 2014, December 8-13 2014, Montreal, Quebec, Canada*, pp. 3320–3328, 2014. URL <https://proceedings.neurips.cc/paper/2014/hash/375c71349b295f5be2dcdca9206f20a06-Abstract.html>.
- Chiyuan Zhang, Samy Bengio, and Yoram Singer. Are all layers created equal? *CoRR*, abs/1902.01996, 2019. URL <http://arxiv.org/abs/1902.01996>.

A Appendix

A.1 Auxiliary plots

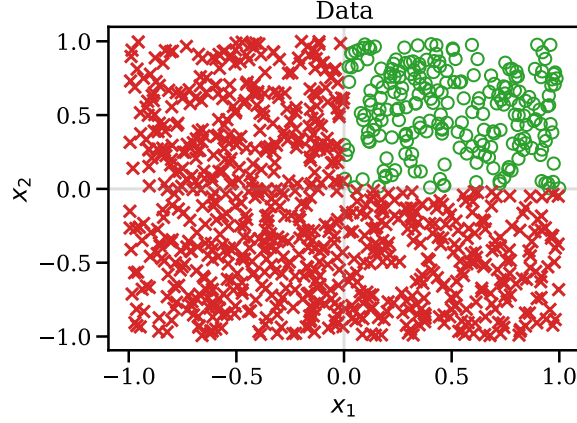


Figure 6: The counterexample classification problem data.

A.2 Failed idea: A method for steepest descent

Imagine standing in weight space at Θ_A and trying to decide in which immediate direction to move in order to approach a Θ_B -equivalent point. There are many, many possible permutations of Θ_B – call them $\pi^{(1)}(\Theta_B), \pi^{(2)}(\Theta_B), \dots$ – to aim for in the distance. Assuming that the loss landscape is in fact (quasi-)convex modulo these permutation symmetries, a natural choice would be to pick the $\pi^{(i)}(\Theta_B)$ that corresponds to the direction of steepest descent starting from Θ_A since we expect $\pi^{(i)}(\Theta_B)$ to lie in the same basin as Θ_A . In other words,

$$\min_{\pi} \left. \frac{d\mathcal{L}(\Theta_A + \lambda(\pi(\Theta_B) - \Theta_A))}{d\lambda} \right|_{\lambda=0} = \min_{\pi} \nabla\mathcal{L}(\Theta_A)^\top (\pi(\Theta_B) - \Theta_A) \quad (6)$$

$$= -\nabla\mathcal{L}(\Theta_A)^\top \Theta_A + \min_{\pi} \nabla\mathcal{L}(\Theta_A)^\top \pi(\Theta_B) \quad (7)$$

Now, we are tenuously in a favorable situation: $\nabla\mathcal{L}(\Theta_A)$ is straightforward to compute, and picking the best π reduces to a matching problem. In particular it is a SOBLAP matching problem of the same form as in Section 3.2. In addition, there is a fast, exact solution for the single intermediate layer case ($L = 2$).

In practice, we found that this method can certainly find directions of steepest descent, but that they are accompanied by high barriers in between the initial dip and $\pi(\Theta_B)$.

A.3 Proof of Lemma 1

To lighten notation we use $\langle \cdot, \cdot \rangle = \langle \cdot, \cdot \rangle_F$ in this section.

Lemma. Given $A, B \in \mathbb{R}^{d \times d}$,

$$\min_{P, Q \text{ perm. matrices}} \langle PAQ^\top, B \rangle$$

is strongly NP-hard and has no PTAS.

Proof. We proceed by reduction from the quadratic assignment problem (QAP) (Koopmans & Beckmann, 1957; Cela, 2013). Consider a QAP,

$$\min_{P \text{ perm. matrix}} \langle PCP^\top, D \rangle$$

for $\mathbf{C}, \mathbf{D} \in \mathbb{R}^{d \times d}$.

Now, pick $\mathbf{A} = \mathbf{C} + \lambda \mathbf{I}$, $\mathbf{B} = \mathbf{D} - \lambda \mathbf{I}$. Then we have,

$$\min_{\mathbf{P}, \mathbf{Q}} \langle \mathbf{P}(\mathbf{C} + \lambda \mathbf{I})\mathbf{Q}^\top, \mathbf{D} - \lambda \mathbf{I} \rangle = \langle \mathbf{P}\mathbf{C}\mathbf{Q}^\top + \lambda \mathbf{P}\mathbf{Q}^\top, \mathbf{D} - \lambda \mathbf{I} \rangle \quad (8)$$

$$= \langle \mathbf{P}\mathbf{C}\mathbf{Q}^\top, \mathbf{D} \rangle - \lambda \langle \mathbf{P}\mathbf{C}\mathbf{Q}^\top, \mathbf{I} \rangle + \lambda \langle \mathbf{P}\mathbf{Q}^\top, \mathbf{D} \rangle - \lambda^2 \langle \mathbf{P}\mathbf{Q}^\top, \mathbf{I} \rangle \quad (9)$$

$$= \langle \mathbf{P}\mathbf{C}\mathbf{Q}^\top, \mathbf{D} \rangle - \lambda \langle \mathbf{P}^\top \mathbf{Q}, \mathbf{C} \rangle + \lambda \langle \mathbf{P}\mathbf{Q}^\top, \mathbf{D} \rangle - \lambda^2 \text{tr}(\mathbf{P}\mathbf{Q}^\top) \quad (10)$$

For sufficiently large λ , the $\text{tr}(\mathbf{P}\mathbf{Q}^\top)$ term will dominate. Letting $\alpha = \max(\max_{i,j} |C_{i,j}|, \max_{i,j} |D_{i,j}|)$, we can bound the other terms,

$$-d^2 \alpha^2 \leq \langle \mathbf{P}\mathbf{C}\mathbf{Q}^\top, \mathbf{D} \rangle \leq d^2 \alpha^2 \quad (11)$$

$$-\lambda d \alpha \leq -\lambda \langle \mathbf{P}^\top \mathbf{Q}, \mathbf{C} \rangle \leq \lambda d \alpha \quad (12)$$

$$-\lambda d \alpha \leq \lambda \langle \mathbf{P}\mathbf{Q}^\top, \mathbf{D} \rangle \leq \lambda d \alpha \quad (13)$$

Now there are two classes of solutions: those where $\mathbf{P} = \mathbf{Q}$ and those where $\mathbf{P} \neq \mathbf{Q}$. We seek to make the best (lowest) possible $\mathbf{P} \neq \mathbf{Q}$ solution to have worse (higher) objective value than the worst (highest) $\mathbf{P} = \mathbf{Q}$ solution. When $\mathbf{P} = \mathbf{Q}$, the highest possible objective value is

$$d^2 \alpha^2 + \lambda d \alpha + \lambda d \alpha - \lambda^2 d$$

and similarly, the lowest possible objective value when $\mathbf{P} \neq \mathbf{Q}$ is

$$-d^2 \alpha^2 - \lambda d \alpha - \lambda d \alpha - \lambda^2 d + \lambda^2$$

where the final term is due to the fact that at least one entry of $\mathbf{P}\mathbf{Q}^\top$ must be 0. With some algebra, it can be seen that $\lambda > 5d\alpha$ is sufficient to guarantee that all $\mathbf{P} = \mathbf{Q}$ solutions are superior to all $\mathbf{P} \neq \mathbf{Q}$ solutions.

Now when $\mathbf{P} = \mathbf{Q}$, all frivolous terms reduce to constants and we are left with the QAP objective:

$$\begin{aligned} \min_{\mathbf{P}} \langle \mathbf{P}\mathbf{C}\mathbf{P}^\top, \mathbf{D} \rangle - \lambda \langle \mathbf{P}^\top \mathbf{P}, \mathbf{C} \rangle + \lambda \langle \mathbf{P}\mathbf{P}^\top, \mathbf{D} \rangle - \lambda^2 \text{tr}(\mathbf{P}\mathbf{P}^\top) \\ = -\lambda \text{tr}(\mathbf{C}) + \lambda \text{tr}(\mathbf{D}) - \lambda^2 d + \min_{\mathbf{P}} \langle \mathbf{P}\mathbf{C}\mathbf{P}^\top, \mathbf{D} \rangle \end{aligned}$$

completing the reduction. QAP is known to be strongly NP-hard (Koopmans & Beckmann, 1957; Sahni & Gonzalez, 1976) and MaxQAP is known to not admit any PTAS (Makarychev et al., 2014), thus completing the proof. \square